

Title	Combined Adaptive RAKE Diversity (ARD) and Coding for DPSK DS/CDMA Mobile Radio
Author(s)	Higashi, Akihiro; Matsumoto, Tadashi
Citation	IEEE Journal on Selected Areas in Communications, 11(7): 1076-1084
Issue Date	1993-09
Type	Journal Article
Text version	publisher
URL	http://hdl.handle.net/10119/4636
Rights	Copyright (c)1993 IEEE. Reprinted from IEEE Journal on Selected Areas in Communications, 11(7), 1993, 1076-1084. This material is posted here with permission of the IEEE. Such permission of the IEEE does not in any way imply IEEE endorsement of any of JAIST's products or services. Internal or personal use of this material is permitted. However, permission to reprint/republish this material for advertising or promotional purposes or for creating new collective works for resale or redistribution must be obtained from the IEEE by writing to pubs-permissions@ieee.org . By choosing to view this document, you agree to all provisions of the copyright laws protecting it.
Description	



Combined Adaptive RAKE Diversity (ARD) and Coding for DPSK DS/CDMA Mobile Radio

Akihiro Higashi, *Member, IEEE*, and Tadashi Matsumoto, *Member, IEEE*

Abstract—A new diversity combining scheme, adaptive RAKE diversity (ARD), is proposed for differential PSK direct sequence code division multiple access (DS/CDMA) mobile communications system. The ARD scheme aims to minimize the mean squared errors in the diversity combiner output. This suppresses the effects of the interference only paths in the time window for path diversity combining. Bit error rate (BER) performances with the proposed ARD and conventional equal gain combining (EGC) schemes are evaluated through laboratory experiments and compared. Block error rate (BKER) performance with the ARD scheme is also evaluated experimentally. Based upon the BKER evaluation results, a new error correction scheme is proposed that is suitable for error occurrence characteristics of ARD output.

I. INTRODUCTION

RECENTLY, the application of code division multiple access (CDMA) spread spectrum techniques to digital mobile communications systems has attracted much attention [1]–[3]. This is because of the possibility of achieving larger capacity than is possible with existing orthogonal multiple access schemes such as time division multiple access (TDMA) and/or frequency division multiple access (FDMA) schemes. In direct sequences (DS) CDMA spread spectrum systems, the same frequency band is shared by many transmitter/receiver pairs. The receiver uses a matched filter corresponding to the reference user's spreading chip sequence. This makes it possible to extract the desired signal components from the composite signal comprised of the desired interference signals.

In mobile radio environments, the received signals are subjected to multipath fading which severely degrades signal transmission performance. If the chip rate $1/T_c$ is higher than the channel coherence bandwidth, where T_c is the chip duration, fading tends to be frequency selective. Because there are many propagation paths with different delay times, the transmitted signal components corresponding to these propagation paths arrive at the receiver at different times [4]. If T_c is smaller than all of the differences in propagation delay time, each of the signal components corresponding to the propagation paths can be resolved in the despreading process. Because the signal components extracted from the received composite signal suffer from independent fading, these can be used as diversity branches. This is the great

advantage of DS/CDMA spread spectrum signaling over conventional orthogonal multiple access schemes and, therefore, receiver systems featuring this path diversity technique have been widely researched previously as the "RAKE" combining system [5]–[7].

Fading environments lead to fast variations in the received signal phase and envelope, and this makes coherent detection very difficult to use. Differential detection requires no carrier recovery function and is, thus, from the practical point of view, promising for mobile radio applications. Therefore, this paper considers DS/CDMA spread spectrum signaling with differential phase shift keying (DPSK).

Even for DPSK, it is still difficult to precisely track the time at which the desired signal components corresponding to a propagation path are received in order to demodulate the desired signals. This is because the propagation profile may vary rapidly and, furthermore, the received signal may suffer from Doppler shifting due to vehicle motion. The post-demodulation integration RAKE (PDI-RAKE) system can solve this problem by setting the time window so that some of the desired demodulated signals are included. The time window position is determined from the detected correlation peak in the despreading process. The PDI receiver requires no accurate path tracking function such as a delay lock loop (DLL) or tau-dither loop (TDL): a simple digital phase locked loop (DPLL) is applicable to this time window positioning technique.

The PDI receiver combines demodulated signals in the time window. If at any of the chips in the time window the demodulator output has no desired signal component, and if these "interference-only paths (IOP's)" are combined with equal weight, the combined received signal quality degrades. This IOP effect on the bit error rate (BER) performance of the PDI-RAKE system was analyzed in [8]–[10]. Reference [8] evaluated the BER performance with the PDI-RAKE system with orthogonal signaling in the presence of IOP's; square-law combining was assumed. Reference [9] also investigates the IOP effect on the BER performance of orthogonal signaling with square-law combining, and an adaptive threshold control scheme that mitigates the IOP effect was proposed. Reference [10] analyzed the path diversity improvement of the PDI-RAKE system with DPSK modulation, in which an exponential delay profile and a fixed time window size was assumed. It was shown in [10] that there is an optimal time window size that minimizes the BER of the PDI-RAKE combiner output, given a fixed value of the channel delay spread.

Manuscript received April 1992; revised November 1992.

The authors are with NTT Mobile Communications Network Inc., Kana-gawaken, 238-03 Japan.

IEEE Log Number 9210919.

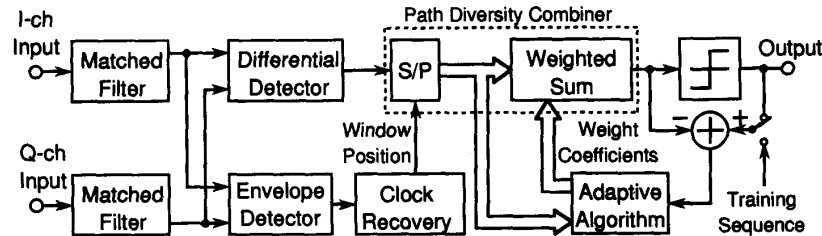


Fig. 1. Block diagram of the ARD receiver.

This paper proposes a new adaptive path diversity combining scheme for PDI reception: adaptive RAKE diversity (ARD). A training sequence is embedded in the information sequence to be transmitted, and used as a reference signal. The demodulated signals in the time window are unequally weighted and combined. The values of the weight coefficients are determined so that the mean square errors in the combiner output are minimized. The ARD system reduces the effects of the IOP and also demodulates desired signals suffering from significant interference power in the time window. It enhances the contributions to the combiner output of demodulated desired signals that experience only slight interference.

A prototype ARD receiver was constructed together with an equivalent baseband laboratory experiment system which, in real time, simulates a broadband fading signal transmission environment. The BER performance of the ARD system was evaluated using the experimental system. The error occurrence characteristic in the ARD receiver output was also analyzed experimentally. A new coding scheme suitable for this characteristic is then proposed, based upon the experimental results. It is shown that, with a small delay time, the proposed scheme exhibits powerful error correction capabilities for ARD output symbol sequences.

This paper is organized as follows. Section II presents the system configuration of the ARD receiver, and analyzes the lower bound of the BER performance of the ARD reception scheme in the additive white Gaussian noise (AWGN) environment. Section III describes the construction of an equivalent baseband laboratory experimental system, and presents experimental results of BER performance evaluations. A comparison between the BER performances with ARD and the conventional equal gain RAKE combining (EGC) schemes is made. Section IV investigates the error occurrence characteristic of the ARD output sequence. Experimental results for block error rate (BKER) with the ARD reception scheme are presented. A new error correction scheme suitable for the ARD system is then proposed. The BER performance with combined ARD and proposed error correction scheme is estimated from the measured BKER performance.

II. ARD RECEPTION SCHEME

A. System Model

Fig. 1 shows a block diagram of the ARD receiver. The input in-phase and quadrature-phase channel components (*I*-ch and *Q*-ch components) are correlated with the reference

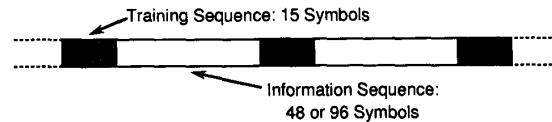


Fig. 2. Frame format.

user's spreading sequence. The correlator output *I*-ch and *Q*-ch signals are fed to the binary DPSK demodulator, where the phase difference between the *I*-ch and *Q*-ch pairs of the correlator output samples separated in time by the information symbol duration is detected each chip interval. The DPSK demodulator output is then input to a path diversity combiner.

The time window size of the path diversity combiner is *M* chips. The chip duration is assumed to be small enough to resolve each propagation path. If the time window size is sufficiently large compared to the channel delay spread, desired signal components corresponding to each propagation path can be combined. However, too wide a time window combines the IOP's. The weight coefficients for diversity combining are determined using an adaptive algorithm so that the mean squared error in the combiner output is minimized. A training sequence is embedded in the transmitted symbol sequence (see Fig. 2), and used as a reference signal for the adaptive algorithm.

The correlation peak position is determined from the correlator output signal envelope. The time window for the ARD reception is positioned so that the desired signal components of the demodulator output signals are included, and shifted gradually to track the desired signals. Time window positioning is performed at the beginning of each training sequence, and the set position is kept until the next training sequence is received.

B. Performance Analysis

In AWGN, the bit error probability $P_b(\gamma)$ at the output of DPSK post demodulation equal gain combining is, without fading, given by [11]

$$P_b(\gamma) = \frac{1}{2^{2M-1}} e^{-\gamma} \sum_{i=0}^{M-1} b_i \gamma^i \quad (1)$$

where *M* is the number of chips in the time window and

$$b_i = \frac{1}{i!} \sum_{j=0}^{M-1-i} \binom{2M-1}{j}. \quad (2)$$

γ is the total equivalent received signal energy per symbol-to-noise power spectral density ratio (E_S/N_0) given by [10]

$$\gamma = \sum_{k=1}^M \gamma_k \quad (3)$$

where γ_k is the received E_S/N_0 for the k th path.

The average BER P_b under fading can be calculated by averaging $p_b(\gamma)$ over the probability density function (pdf) $p(\gamma)$ of γ as

$$P_b = \int_0^{\infty} p_b(\gamma)p(\gamma) d\gamma. \quad (4)$$

Assuming that all γ_i 's corresponding to each chip are statistically independent, the characteristic function approach can be used to derive $p(\gamma)$. Let the Laurent series expansion of the characteristic function $F(s)$ of γ be denoted as [19]

$$F(s) = \sum_{j=0}^{\infty} a_j s^{-j} \quad (5)$$

where a_j 's are the residues of $F(s)$. The pdf $p(\gamma)$ of γ can then be expressed as

$$p(\gamma) = \sum_{j=0}^{\infty} a_j \frac{\gamma^{j-1}}{(j-1)!}. \quad (6)$$

If there are m propagation paths having equal path gain,

$$a_j = 0, \quad j = 0, 1, \dots, m-1 \quad (7a)$$

and the next two residues, a_m and a_{m+1} , are given by

$$a_m = \frac{1}{\Gamma^m} \quad (7b)$$

$$a_{m+1} = \frac{m}{\Gamma^{m+1}} \quad (7c)$$

where Γ is the average E_S/N_0 on each propagation path. Substituting (1) and (6) into (4) yields

$$P_b = \frac{1}{2^{2M-1}} \sum_{i=0}^{M-1} \sum_{j=m}^{\infty} a_j b_i \frac{(i+j-1)!}{(j-1)!} \quad (8)$$

Taking two terms of a_m and a_{m+1} , we have

$$P_b \simeq \frac{1}{2^{2M-1}} \frac{1}{\Gamma^m (m-1)!} \sum_{j=0}^{M-1} \cdot b_j \left\{ (m+j-1)! - \frac{1}{\Gamma} (m+j)! \right\}. \quad (9)$$

Fig. 3 shows the calculated average BER versus $m\Gamma$, where for any value of m , the $m\Gamma$ value has been kept constant since the transmitted signal power is divided into m paths.

It is found from Fig. 3 that, with the double-spike delay profile, the average BER of the EGC scheme with $M = 6$ is 1.6 dB worse than that with $M = 2$. It is obvious that, in the AWGN environment, the BER performance of the EGC scheme with $M = 2$ lowerbounds that of the ARD scheme with $M \geq 3$ for the double-spike delay profile. Because of

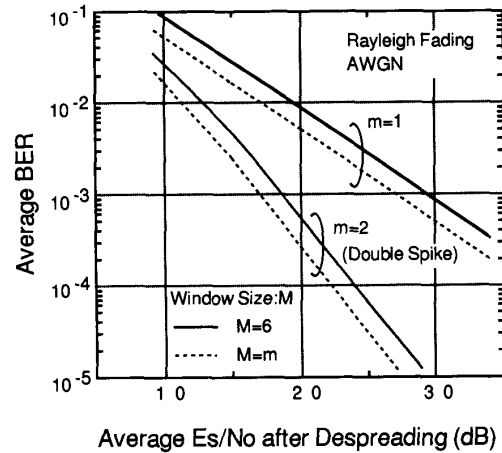


Fig. 3. Theoretical average BER versus average E_S/N_0 .

the imperfect tracking performance of the adaptive algorithm used in ARD reception, this lower bound may not be reached in a practical receiver. This will be experimentally examined in the next section.

III. EXPERIMENTAL SYSTEM

A major factor that dominates signal transmission performance is interference because, in DS/CDMA communications systems, the same frequency band is shared by many transmitter receiver pairs. This makes it very difficult to estimate the signal transmission performance of a DS/CDMA system because, unless a lot of real transmitter receiver pairs are field or laboratory tested, the actual performance cannot be evaluated. Determining the effects of interference can be simplified by assuming that the composite signal of many interference signals is additive white Gaussian noise. However, this assumption creates a too-optimistic estimation.

In order to reduce this difficulty, and to improve the accuracy of performance evaluations through laboratory experiments, an equivalent baseband experiment system was built. The system allows, in real time, the simulation of broadband fading signal transmission environments. Also, a prototype of the ARD receiver was constructed. This section introduces the experimental system, and presents experimental results for BER performance evaluations of the ARD and EGC schemes.

A. ARD Prototype

Fig. 2 shows the frame format used in the prototype. The training sequence is 15 symbols long, and the information sequence is either 48 or 96 symbols long. In the transmitter, the training and information sequences to be transmitted are differentially encoded and multiplied by the spreading sequence. The chip rate ($1/T_c$) was 1.024 Mb/s, and the symbol rate ($1/T_s$) before spreading was 8.063 ($= 1024/127$) kb/s. Gold codes with a length of 127 chips were used for the spreading sequence (process gain is 21 dB). The spread chip stream was then fed to the equivalent baseband channel simulator.

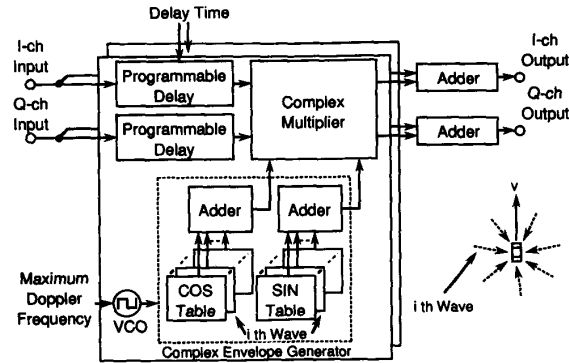


Fig. 4. Block diagram of the equivalent baseband frequency selective multi-path fading simulator.

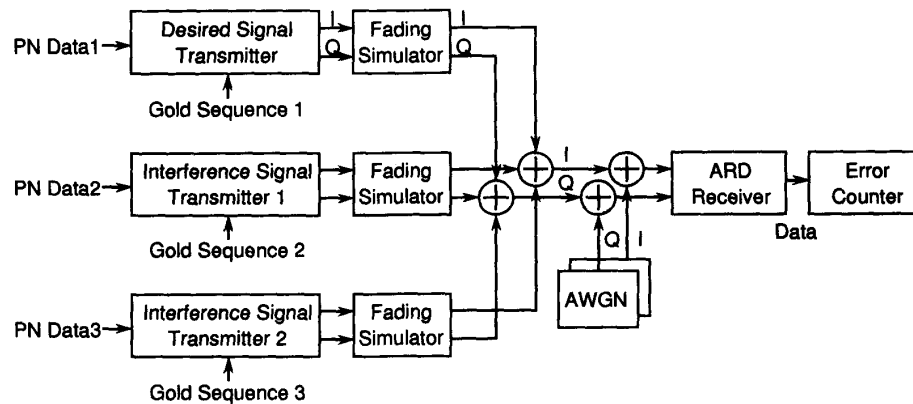


Fig. 5. Block diagram of the experiment system.

Two Plessey matched filter IC's, PDSP16256, were used as I -ch and Q -ch despreaders. Another Plessey IC, PDSP16116, was used to calculate $I^2 + Q^2$. The peak position detector was constructed with random logic circuitry. The I -ch and Q -ch outputs and detected peak position were then input to a Motorola DSP96000, which performed the ARD algorithm with a window size of 6. For ARD combining, the RLS (recursive least squares) algorithm was used for both the training and information sequences. Moreover, time window positioning was performed on the DSP using a conventional DPLL algorithm.

B. Channel Simulator

Fig. 4 shows the block diagram of the equivalent baseband fading simulator. The double-spike model was employed as the channel delay profile. The two propagation paths were assumed to have equal gain. The input I -ch and Q -ch components were sampled at a sampling interval of $1/4.096$ MHz asynchronous to the input chip timing. The input sample sequence was replicated to simulate a propagation environment having the double-spike delay profile.

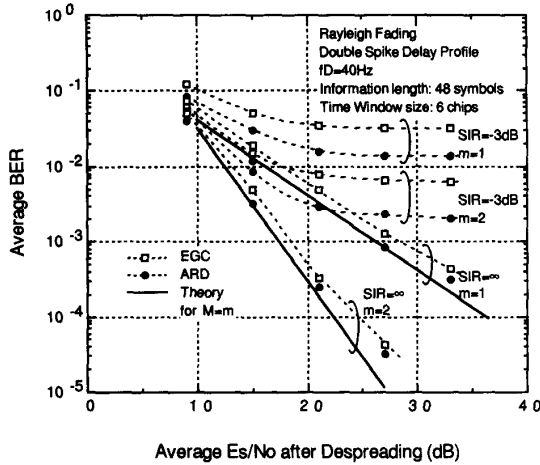
Two I -ch and Q -ch pairs of the complex fading envelope were generated based on the model described in [12]. The input sample sequence was multiplied by one of these two

pairs in the complex domain. The delayed version of the input sample sequence was multiplied by the other pair in the complex domain. These were then summed up, and the resulting I -ch and Q -ch samples were the output of the fading simulator. The maximum Doppler frequency can be set independently of the input chip rate within the range of 1 Hz to 400 Hz (*step size* = 1 Hz). The adjustable range of the delay spread is from $0 \mu\text{s}$ to $31 \mu\text{s}$ (*step size* = 250 ns).

Fig. 5 shows the block diagram of the laboratory experimental system. One desired and two interference complex signals, each of which suffers from independent frequency-selective Rayleigh fading generated by the baseband fading simulator, and two-dimensional (I -ch and Q -ch components) AWGN are combined in the complex domain by two four-input full adders. Assuming a Nyquist receive filter, the resulting signals are then brought to the prototype ARD receiver. In the experiments, these signals were assumed to have identical chip timing but different symbol timing.

C. BER Performance Evaluations

Laboratory experiments were conducted to evaluate the BER performances of the ARD and EGC schemes using the equivalent baseband laboratory experiment system. The spreading sequences were randomly selected from among

Fig. 6. Average BER versus average E_S/N_0 .

the Gold codes and assigned to the interference signals, so that the effect of cross correlation between the desired and interference spreading sequences could be averaged over the sequences of the Gold codes.

Fig. 6 shows the experimental results for average BER's with ARD and EGC schemes for infinite and -3 dB signal-to-interference power ratio (SIR) values, and the information symbol sequence length of 48 symbols versus the average received E_S/N_0 ($= m\Gamma$) after despreading with the number m of propagation paths as a parameter. The path gain for $m = 2$ was set at one-half of that for $m = 1$. The theoretical BER's calculated from (9) for the infinite SIR are also plotted for $m = 1$ and $m = 2$ with the time window size M of $M = m$. It is found from this figure that because several chips do not include any desired signal components in the time window, the average BER of the EGC scheme is worse than that of the ARD scheme. The experimental results of the ARD scheme with $m = 6$ agree well with theoretical BER with $M = m$. This implies that the ARD scheme can suppress the effect of such chips on BER performance. When the average SIR is -3 dB, average BER decreases as average E_S/N_0 increases; however, the BER values reach a floor determined by the -3 dB average SIR. Nevertheless, the ARD scheme can achieve better BER performance than the EGC scheme for all average E_S/N_0 values.

Fig. 7 shows the average BER of the ARD and EGC reception schemes versus the maximum Doppler frequency f_D for an infinite average E_S/N_0 and the average SIR of -3 dB. It is found that the average BER of the EGC scheme is almost insensitive to the f_D value. The average BER of the ARD schemes degrades as f_D increases. This occurs because, at high f_D values, the number of embedded training sequences is insufficient.

IV. CHANNEL CODING

Several channel coding schemes for the DS/CDMA communication systems have been previously proposed, and their performances have been analyzed [13]–[15]. Most of these

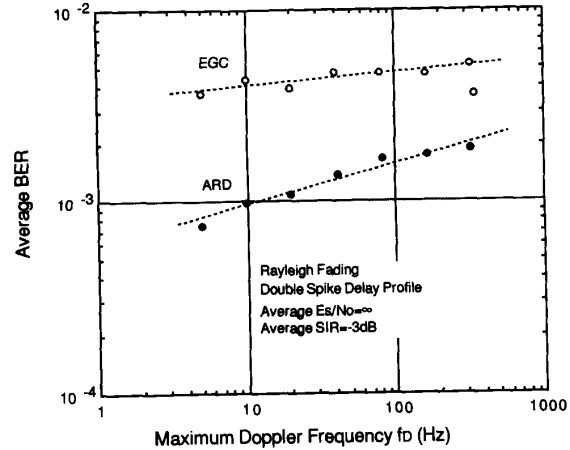


Fig. 7. Average BER versus maximum Doppler frequency.

coding schemes assume perfect interleaving, where the interleaving degree is assumed to be sufficiently large to randomize errors occurring in the received symbol sequence. However, this assumption is not always reasonable because the delay time caused by interleaving must be within an acceptable limit and, therefore, burst errors may not be perfectly randomized.

This section describes experimental results for the block error rate (BKER) performance of ARD reception. A new channel coding scheme is proposed which does not use interleaving. Nevertheless, it exhibits a powerful error correction on the ARD output symbol stream.

A. BKER Performance

$BKER_1(N, t)$ is defined as the probability that more than t symbols among an N -symbol block are received in error. $BKER_1(N, t)$ can be expressed as

$$BKER_1(N, t) = 1 - \sum_{i=0}^t bker_1(N, i) \quad (10)$$

where $bker_1(N, i)$ is the probability that i symbols in a transmitted N -symbol block are received in error. $BKER_1(192, t)$ and $BKER_1(96, t)$ were evaluated through the experimental system described in Section III. As shown in Fig. 8, the code word consists of either two consecutive information symbol sequences or the pairs of every other sequence. For convenience, the former is called consecutive structuring, the latter is termed interframe structuring. Fig. 9 shows $BKER_1(96, t)$ and $BKER_1(192, t)$ versus the values of t for the average SIR of -3 dB and the average E_S/N_0 's of 9 dB and 15 dB. Fig. 9(a) shows $BKER_1(96, t)$, and Fig. 9(b) shows $BKER_1(192, t)$. It is found from Fig. 9(a) that, even for the average E_S/N_0 of 15 dB, $BKER_1(96, t)$ does not decrease rapidly when $20 \leq t \leq 40$, and $BKER_1(96, 40)$ remains at about 10^{-3} . However, when $t \geq 48$ ($= 96/2$), $BKER_1(96, t)$ drops rapidly from the value of 10^{-3} . A similar characteristic is seen in Fig. 9(b); for $40 \leq t \leq 90$, $BKER_1(192, t)$ decreases slowly, and for $t \geq 96$ ($= 192/2$) $BKER_1(192, t)$

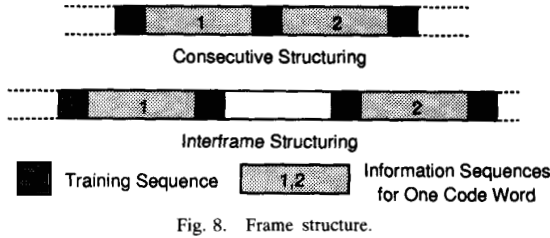


Fig. 8. Frame structure.

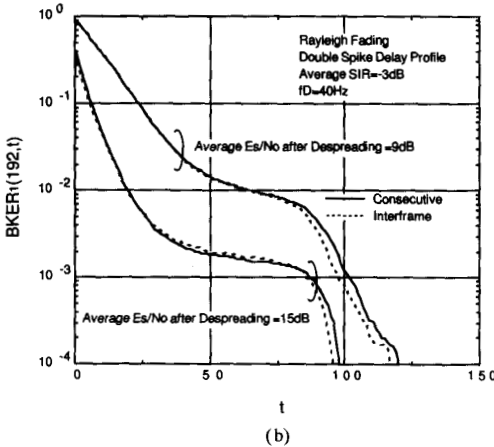
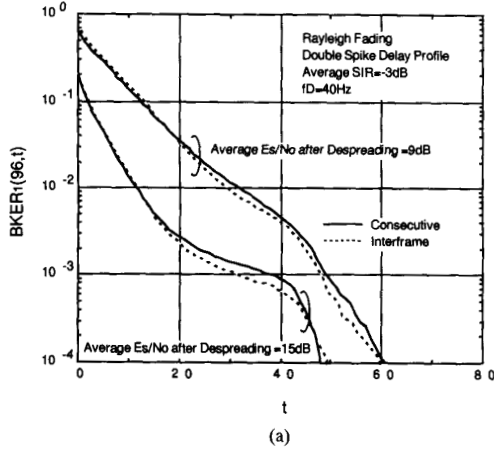


Fig. 9. $BKER_1$ versus t . (a) $BKER_1(96, t)$. (b) $BKER_1(192, t)$.

drops rapidly. BKER performance with interframe structuring is almost equivalent to that with consecutive structuring.

These observations suggest that errors in the ARD output sequence are quite bursty, and clustered errors in the information symbol sequence are likely. This is reasonable because if, during the training sequence, the values of the weight coefficients determined by the RLS algorithm used for ARD reception are the optimum to minimize the IOP effect, the subsequent information symbol sequence suffers only from AWGN. However, if a deep fade corrupts the entire training sequence, the values of the weight coefficients may differ widely from their optimal values. In this case, burst errors

with a length almost the entire information symbol sequence are possible.

B. New Error Correction Scheme

A new error correction scheme is proposed that usefully employs the error occurrence characteristic in the ARD output sequence. Two codes, C_1 and C_2 , are used in the proposed scheme. C_1 is a small redundancy code for error detection, and C_2 is a half-rate code for error correction. The input information symbol stream to be transmitted is segmented into blocks, each of which has a length of k symbols. These blocks are first encoded with the C_1 code. The C_1 -coded information block is referred to as the I part for convenience. The I part is then encoded with the half-rate C_2 code. Therefore, the total code rate of this coding scheme is $k/2n$. The check symbols of the C_2 code have length n . This check part of the C_2 code is referred to as the C part. The C_2 code realizes not only random error correction but also code invertibility [16]: the equations $C = GI$ and $I = G^{-1}C$ hold where the $n \times n$ matrix G is nonsingular.

The I and C parts are transmitted using the frame format depicted in Fig. 8. The receiver first examines the received I part. If the C_1 code detects no error in the received I part, its k information symbols are delivered to the data sink. If the received I part is detected in error, the receiver analyzes the received C part. Another I part is calculated from the received C part using $I = G^{-1}C$. If the C_1 code detects no error in the calculated I part, its k information symbols are delivered to the data sink. If the calculated I part is detected in error, t -symbol error correction is applied to the received word comprised of the I and C parts, where t is the error correction capability of the $(2n, n)$ invertible code. If the C_1 code detects no error in the decoded I part, the k information symbols in the decoded I part are then picked up and delivered to the data sink. If the decoded I part is again detected in error, the k information symbols in the received unprocessed I part are output.

This error correction scheme does not use interleaving, and incurs an acceptable amount of delay. Even when interframe structuring is applied, the delay time of this error correction scheme is $3 \times Ts \times (n + \text{length of the training sequence})$, where Ts is the information symbol duration. This is the great advantage of this scheme over the conventional coding schemes based on interleaving. With this decoding scheme, errors that are larger than t symbols can be corrected if either the I or C part has no error. From the BKER analysis in Section IV-A, this event is found to be likely. Therefore, the proposed scheme is expected to exhibit powerful error correction.

Fig. 10 shows the block error probability $BKER_2(N, t)$, given that both the received I and C parts are received in error and that the number of errors occurring in the composite received word is more than t . The double-spike delay profile was assumed. Fig. 10 (a) is for $2N = 96$, and Fig. 10(b) is for $2N = 192$. It is found from these figures that, for average $E_S/N_0 = 15$ dB, the proposed scheme can greatly reduce the BKER values. If interframe structuring is applied, the BKER values can be further reduced. This feature is not observed in

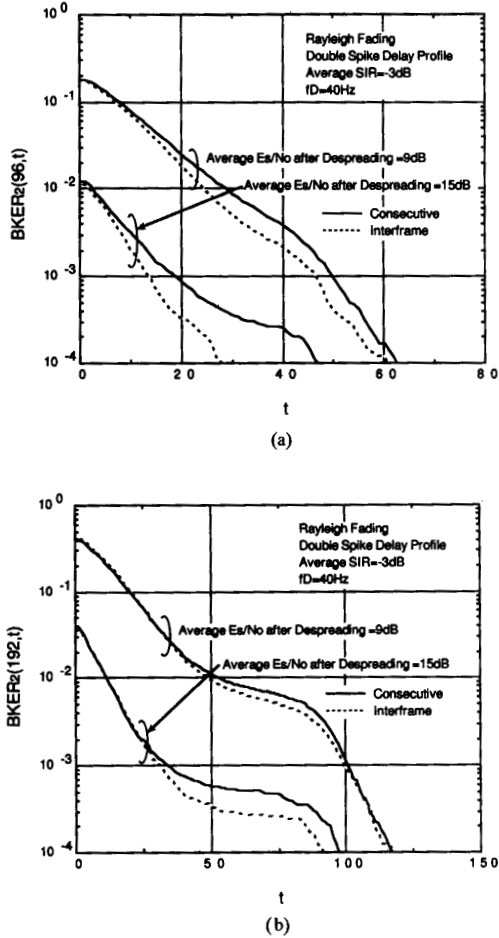


Fig. 10. BKER₂ versus t. (a) BKER₂(96, t). (b) BKER₂(192, t).

BKER performance with the random error correction scheme, even when interframe structuring was applied.

C. BER Performance after Decoding

An acceptable approximation formula for random error correction block codes to estimate the BER after decoding is [17]

$$BER \approx \frac{2t+1}{N} \sum_{i=t+1}^{2t+1} bker_1(N, i) + \frac{1}{N} \sum_{i=2t+2}^N i \cdot bker_1(N, i). \tag{11}$$

The BER after decoding of (96, 48) and (192, 96) codes were calculated using (11). Fig. 11 shows the BER's after decoding of (96, 48) and (192, 96) codes versus the average E_S/N_0 with the average SIR of -3 dB. The double-spike delay profile was assumed. Fig. 11(a) is for the (96, 48) code, and Fig. 11(b) is for the (192, 96) code. The error correction capability of each code, t, was chosen as the largest integer value that satisfies the Hamming bound [18]. t = 11 for (96, 48) and t = 22 for (192, 96) codes.

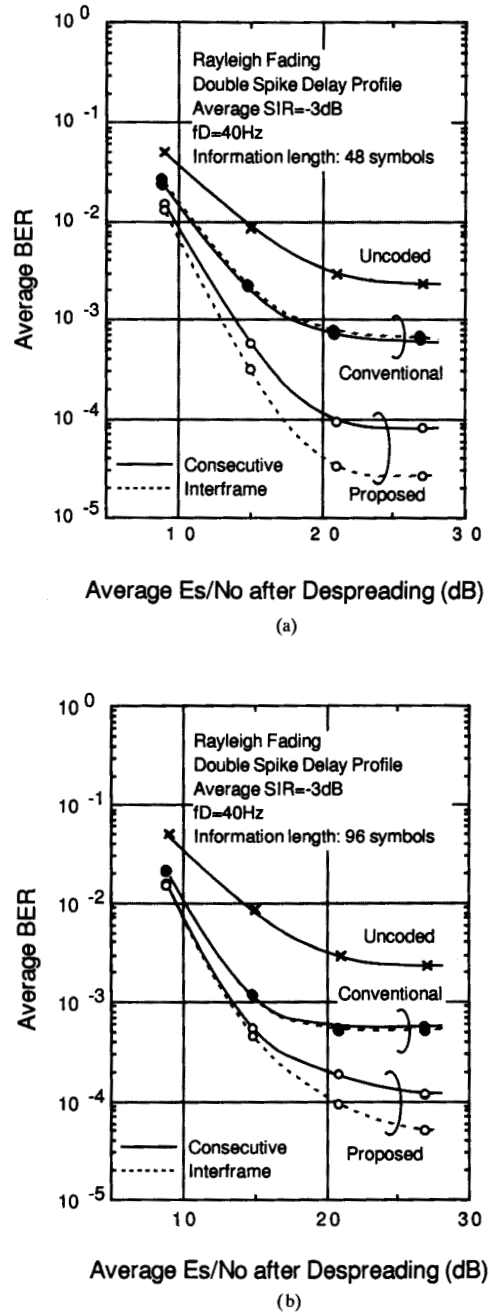


Fig. 11. Average BER versus average E_S/N_0 . (a) Information length of 48 symbols. (b) Information length of 96 symbols.

The BER performance with the proposed coding scheme can be estimated from

$$BER \approx \frac{1}{N} \sum_{i=t+1}^N i \cdot bker_2(N, i) \tag{12}$$

where $N = 2n$ and $bker_2(N, i)$ is the probability that both of the received I and C parts are received in error and the

number of errors occurring in the composite received word is i . Fig. 11 also shows the BER's of the proposed error correction scheme. It was assumed that the $(n, n-16)$ cyclic redundancy code is used for the C_1 code, and that this code can detect all error patterns. It is found from this figure that the proposed scheme with consecutive structuring can achieve a coding gain at $\text{BER} = 3 \times 10^{-3}$ of about 5 dB with length 96 code and 6 dB with length 192 code, where the bandwidth expansion factor due to coding is taken into account. The coding gain can be further, but only slightly, increased with interframe structuring. When the conventional random error correction scheme with either consecutive or interframe structuring is used, the gain at $\text{BER} = 3 \times 10^{-3}$ is about 4 dB for length 96 code and 5 dB for length 192 code. It is also found from this figure that the proposed scheme is effective in lowering the error floor due to the -3 dB average SIR. More than one decade reduction in the BER floor is observed for both 96 and 192 length codes.

V. CONCLUSIONS

A new diversity combining scheme, adaptive RAKE diversity (ARD), for DS/CDMA mobile radio communications systems with DPSK modulation has been proposed. The ARD reception scheme combines the demodulated signals in the time window, like other conventional PDI-RAKE combining schemes; however, the weight coefficients for combining are determined so that the mean squared error in the combiner output is minimized. This reduces the effects of not only the interference-only paths (IOP's) in the time window but also the effect of the demodulated signals suffering from large interference. This scheme enhances the contribution of the demodulated signals experiencing only slight interference to the combiner output.

A prototype ARD receiver was constructed. The BER performance of the ARD scheme was evaluated using a laboratory experimental system. It was shown that in the double-spike propagation environment with infinite average SIR, the prototype ARD receiver with window size of 6 (thus suffering from four chips having no desired signal components) can achieve a BER performance almost equivalent to that of two branch EGC diversity reception.

The BKER performance of the ARD scheme was also analyzed experimentally. Based upon experimental results, a new error correction scheme suitable for the error occurrence characteristic of the ARD output was then proposed. Code invertibility and error correction capability are strategically used. It has been shown that the proposed scheme exhibits powerful error correction on the ARD output sequence. The proposed scheme is also effective in lowering the BER floor due to the negative SIR values typically encountered in DS/CDMA communications systems.

REFERENCES

- [1] K. S. Gilhousen, I. M. Jacobs, R. Padovani, A. J. Viterbi, A. Weaver Jr., and C. E. Wheatley, "On the capacity of a cellular CDMA system," *IEEE Trans. Vehic. Technol.*, vol. VT-40, no. 2, pp. 303-312, May 1991.
- [2] R. L. Pickholtz, L. B. Milstein, D. L. Schilling, M. Kullback, D. Fishman, and W. H. Biederman, "Field tests designed to demonstrate increased

spectral efficiency for personal communications," *Conf. Rec. IEEE Globecom '91*, Phoenix, AZ, Dec. 1991, pp. 26.1.1-26.1.5.

- [3] G. R. Cooper and R. W. Nettleton, "A spread spectrum technique for high capacity mobile communications," *IEEE Trans. Vehic. Technol.*, vol. VT-27, no. 4, pp. 264-275, Nov. 1978.
- [4] W. C. Lee, "Overview of cellular CDMA," *IEEE Trans. Vehic. Technol.*, vol. VT-40, no. 2, pp. 291-302, May 1991.
- [5] G. L. Turin, "Introduction to spread-spectrum antimultipath techniques and their application to urban digital radio," *Proc. IEEE*, vol. 68, no. 3, pp. 328-353, Mar. 1980.
- [6] M. Kavehrad and B. Ramamurthi, "Direct-sequence spread spectrum with DPSK modulation and diversity for indoor wireless communications," *IEEE Trans. Commun.*, vol. COM-35, no. 2, pp. 224-236, Feb. 1987.
- [7] U. Grob, A. L. Welti, E. Zollinger, R. Kung, and H. Kaufmann, "Microcellular direct-sequence spread-spectrum radio system using N-path RAKE receiver," *IEEE J. Select. Areas Commun.*, vol. SAC-8, no. 5, pp. 772-780, June 1990.
- [8] J. G. Proakis, *Digital Communications*. New York: McGraw-Hill, 1989, pp. 728-739.
- [9] G. T. Chyi, J. G. Proakis, and C. M. Keller, "Diversity selection/combining schemes with excess noise-only diversity receptions over a Rayleigh-fading multipath channel," *Proc. Conf. Inform. Sci. Syst.*, Princeton Univ., Princeton, N.J., Mar. 1988, pp. 420-425.
- [10] I. K. Chang, G. L. Stuber, and A. M. Bush, "Performance of diversity combining techniques for DS/DPSK signaling over a pulse jammed multipath fading channel," *IEEE Trans. Commun.*, vol. COM-38, no. 10, pp. 1823-1834, Oct. 1990.
- [11] J. G. Proakis, *Digital Communications*. New York: McGraw-Hill, 1989, pp. 298-303.
- [12] W. C. Jakes, Jr., *Microwave Mobile Communications*. New York: Wiley, 1974, pp. 70-76.
- [13] J. K. Omura and B. K. Levitt, "Coded error probability for antijam communication systems," *IEEE Trans. Commun.*, vol. COM-30, no. 5, pp. 896-903, May 1982.
- [14] M. Kavehrad and P. J. McLane, "Performance of low-complexity channel coding and diversity for spread spectrum in indoor, wireless communication," *AT&T Tech. J.*, vol. 64, no. 8, pp. 1927-1965, Oct 1985.
- [15] K. H. Li and L. B. Milstein, "On the process gain of a block-coded direct sequence spread-spectrum system," *IEEE J. Select. Areas Commun.*, vol. SAC-7, no. 4, pp. 618-626, May 1989.
- [16] S. Lin and D. J. Costello, Jr., *Error Control Coding: Fundamentals and Applications*. Englewood Cliffs, NJ: Prentice-Hall, 1983, pp. 481-483.
- [17] F. Adachi and K. Ohno, "BER performance of QDPSK with postdetection diversity reception in mobile radio channels," *IEEE Trans. Vehic. Technol.*, vol. VT-40, no. 1, pp. 237-249, Feb 1991.
- [18] A. M. Michelson and A. H. Levesque, *Error-Control Techniques for Digital Communications*. New York: Wiley, 1985, pp. 94-96.
- [19] M. Schwartz, W. R. Bennett, and S. Stein, *Communication Systems and Techniques*. New York: McGraw-Hill, 1966, pp. 440-453.



Akihiro Higashi received the B.S. and M.S. degrees in electrical engineering from Tokyo Metropolitan University, Hachioji-shi, Japan, in 1985 and 1987, respectively.

Since joining NTT, Yokosuka, Japan, in 1987, he has conducted research in the area of adaptive equalizers for high-speed digital mobile radio applications. Since February 1991, he has been researching DS and/or FH spread-spectrum signal transmission techniques. His current interest includes design and performance evaluation of CDMA mobile communications systems, diversity reception techniques, and interference cancellation and coding. He is currently a Research Engineer at NTT Mobile Communications Network Inc.



Tadashi Matsumoto received the B.S., M.S., and doctorate degrees in electrical engineering from Keio University, Yokohama-shi, Japan, in 1978, 1980, and 1991, respectively.

From 1980 to June 1992, he was with the Nippon Telegraph and Telephone Corporation. (NTT). He participated in the R&D project of NTT's High Capacity Mobile Communication System, where he was responsible for the development of the base station transmitter/receiver unit. From 1987 to February 1991, he was involved in the development of facsimile and data communications service units for the Japanese TDMA digital cellular mobile communications system. In July 1992, he transferred to NTT Mobile Communications Network Inc., Yokosuka-shi, where he is currently a Senior Research Engineer. Since February 1991, he has been researching spread spectrum communications systems and their applications to mobile radios. Since October 1992, he has served as a part-time lecturer at Keio University. His current research interests include DS and/or FH CDMA technologies, multiuser channel detection techniques, modulation/demodulation, and error control strategies for digital mobile radio systems such as FEC's and/or ARQ's.